

## Calculating the Field Emission Current from a Carbon Nanotube

P. VON ALLMEN (a), L. R. C. FONSECA (b), and R. RAMPRASAD (b)

(a) *Motorola Advanced Display Technology Laboratory, Tempe, AZ, USA*

(b) *Motorola Digital DNA Laboratory, Tempe, AZ, USA*

(Received April 1, 2001; accepted May 1, 2001)

Subject classification: 73.63.Fg; 79.90.+q; S5

The purpose of this work is to present elements of a design tool for field emission displays using carbon nanotubes as emitters. We use a continuum model to describe the carbon nanotubes and we use a locally one-dimensional approximation to calculate the emission current. We investigate the emission current to voltage characteristic, screening effects and the lateral spread of the emission current as a function of the height and radius of the nanotube. We also present a set of results pertaining to the electrostatic properties of a carbon nanotube immersed in a uniform electric field. We show that the field enhancement factor at the apex of the nanotube increases linearly with the aspect ratio in the parameter region of interest to field emission applications. We have also found that the relative variation of the field enhancement factor along the cap of the nanotube only depends on the radius and not on the height of the nanotube.

### 1. Introduction

Films containing carbon nanotubes (CNT) are presently used in several industrial attempts to build bright, reliable and cost-effective field emission displays (FED) [1]. One of the favored fabrication techniques is Hot Filament Chemical Vapor Deposition (HF-CVD) because the intrinsic specificity of the catalytic growth allows for effective patterning procedures. However, CNT grown by catalytic CVD at low temperature on glass substrates currently contain a large density of defects and impurities. In some instances, the structures are more similar to graphitic nanofibers than MWNT or SWNT. Furthermore, it is not clear yet precisely which structures contribute to field emission. Despite these multiple unknowns about the exact nature of the emission sites, simulations of field emission properties of these materials are necessary tools for the efficient design of FEDs.

Field emission properties can be calculated at many levels of sophistication. It is throughout conceivable to perform a full quantum transport calculation at the atomic level based e.g. on the non-equilibrium Green's function formalism including a range of scattering mechanisms. However, since the exact atomic structure of the emitter is not known, we feel that such effort would not significantly contribute to an efficient design tool. For similar reasons, we also believe that solving the full 3D scattering problem in a single-particle picture is not needed in a first step. We have therefore opted for two approximate methods that will allow us to qualitatively understand trends in field emission properties such as the current–voltage characteristic, the lateral spread of the emitted electrons, screening effects and field emission microscope (FEM) patterns.

The first method is the electrostatic continuum model, where the CNT is described by a metallic cylinder capped with a hemisphere. The second approach is based on the Bardeen transfer Hamiltonian technique [2] and uses the stationary solutions to the

Schrödinger equation to evaluate the emission current. The latter method allows for an atomic level calculation whereas the former one approximates the CNT with a continuum. In the following sections we will describe the electrostatic continuum model and present some illustrative results. We have described the Bardeen transfer Hamiltonian method more in detail in Ref. [3] and further work is still in a development stage.

## 2. The Electrostatic Continuum Model

As mentioned earlier, we approximate the CNT with a perfectly conductive cylinder with a hemispherical cap. We believe that this approximation will capture the essence of the electrostatic features that would also result from more sophisticated calculations. We will study trends in the current–voltage characteristic, in the spread of the emission current and in the screening effects as the height and radius of the CNT are varied.

The emission of the electrons is determined by the electric field distribution around the CNT. As mentioned in earlier works [4], the barrier width and shape vary along the cap where most of the emission is taking place. In order to calculate the field emission current the first step is therefore to solve the electrostatic boundary value problem. We have chosen the boundary element method, which is well suited for systems with large aspect ratios.

The boundary element method is based on Green’s theorem in 3D and the electrostatic potential  $\Phi(r)$  is given by the following expression:

$$\Phi(r) = \oint_{\partial\Omega} (d\sigma' \cdot \nabla' \Phi(r')) G(r, r') - \oint_{\partial\Omega} (d\sigma' \cdot \nabla' G(r, r')) \Phi(r'),$$

$$G(r, r') = \frac{1}{4\pi|r - r'|},$$

where  $G(r, r')$  is the 3D Green’s function for the Laplace equation. The boundary of the simulation cell  $\partial\Omega$  is then discretized by using the Delaunay triangulation algorithm [5] and the above equation becomes an algebraic expression. If  $r$  is taken on the boundary  $\partial\Omega$  and if we use Dirichlet boundary conditions, the electric field on the boundary is obtained by solving a set of linear equations. Once the electric field is known on the boundary, the electrostatic potential at any location within the simulation cell is given by a summation over the boundary elements.

In principle, the emission current within the single-particle framework is obtained from the 3D scattering matrix. However, since the emission is mainly occurring in the apex region of the cap we believe that a locally 1D approximation will yield meaningful results. Within this approximation, the current at each boundary element is computed according to the following expression:

$$I_n = \int_{E_c}^{\infty} T_n(E) F(E) dE,$$

where  $F(E)$  and  $T_n(E)$  are the supply function and the transmission coefficient, respectively. The total emission current is obtained by summing the contributions of all boundary elements.

We use the following supply function, which is identical to the one for a flat metallic surface:

$$F(E) = \frac{emk_B T}{2\pi^2 \hbar^3} \ln \left( 1 + e^{\frac{E-\mu}{k_B T}} \right).$$

In this model, the CNT is described by a parabolic band with mass  $m$  and band edge  $E_c$  and by a chemical potential  $\mu$ . Such a description neglects peculiarities of the CNT density of states that, however, are only incompletely known for the emitters in a FED film. We therefore believe that this model is sufficiently accurate to calculate the trends mentioned in the Introduction.

The transmission coefficient  $T_n(E)$  for each boundary element is obtained from the solution of the 1D Schrödinger equation with open boundary conditions. The potential barrier is obtained by calculating the electrostatic potential along the direction perpendicular to the boundary element. The numerical method is described in Ref. [6].

The image charge potential is introduced within the following approximations. For a flat metallic surface it is well known that the classical image charge potential contributes a  $-e^2/16\pi\epsilon_0(x+x_0)$  term to the potential energy barrier, where  $x_0$  is the location of the plane defining the image charge distribution. For a curved surface, the image charge effect is reduced and in general no analytical expression is available. In order to assess the effect of curvature we will compare calculations using the flat surface potential with calculations using the image potential for a sphere of radius  $R$ , which is given by the following expression [7]:

$$\Phi_{\text{im}}(r) = -\frac{Re^2}{8\pi\epsilon_0(r^2 - R^2)}.$$

### 3. Results and Discussion

As mentioned in the Introduction, we will present a set of results that determine trends when the height  $H$  and radius  $R$  of the CNT are varied. Figure 1 displays the maximum field enhancement factor as a function of the aspect ratio  $H/R$ . The maximum field enhancement factor  $\beta_{\text{max}}$  is defined as the ratio of the field at the apex of the CNT to the parallel plate field, which is the ratio of the voltage drop between the lid and the bottom of the simulation box divided by the height of the box. We see that  $\beta_{\text{max}}$  increases linearly with the aspect ratio with a slope 0.6. The linear behavior is expected

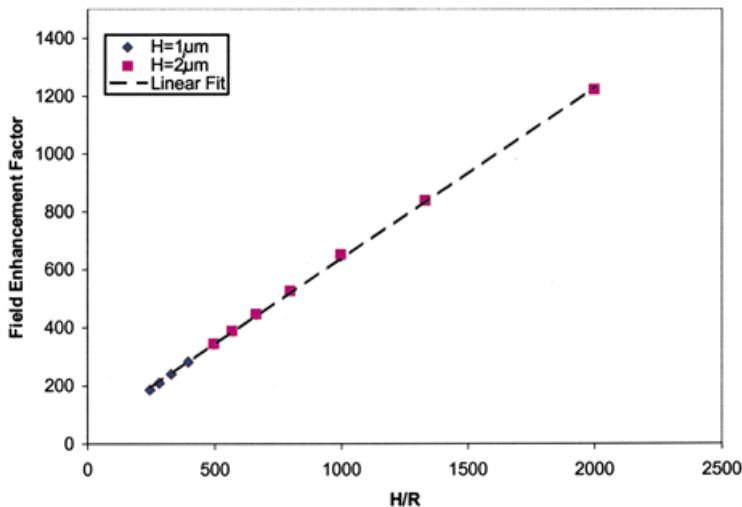


Fig. 1. Field enhancement factor as a function of the aspect ratio. The slope of the linear fit is 0.6

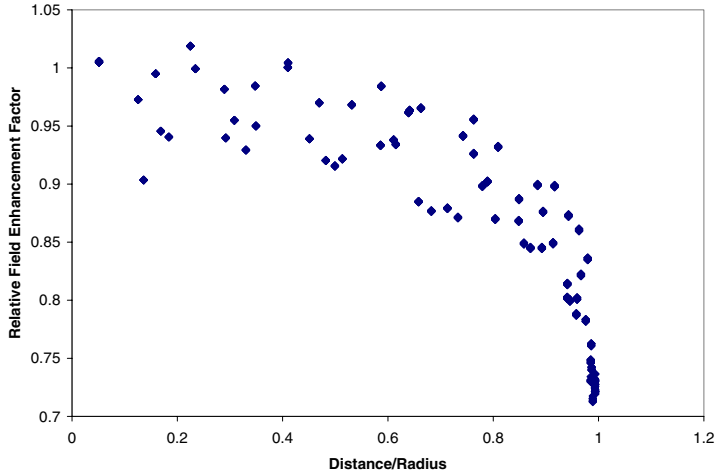


Fig. 2. Relative field enhancement factor as a function of the distance to the axis of the CNT

to be valid only for midrange values of the aspect ratio, which is the relevant region for most field emission applications.

Figure 2 shows the relative variation of the field enhancement factor as a function of the distance to the axis of the CNT scaled by the radius. Each dot represents the field enhancement for one boundary element on the cap. The scattering of the results is a numerical artifact due in part to the unequal sizes of the elements. We found that the shape of the curve does not depend on the height of the CNT within the range of aspect ratios considered in Fig. 1. We observe that the decrease from the apex to the edge of the cap is approximately 30%. Since the dependence of the emission current on the electric field is exponential the current emitted by boundary elements at the edge of the cap is several orders of magnitude smaller than the current at the apex.

Figure 3 displays the potential barrier (with and without image charge potential) plotted perpendicularly to the apex of a typical CNT. As already pointed out by several authors [4], the magnitude of the electric field, which is the negative derivative of the

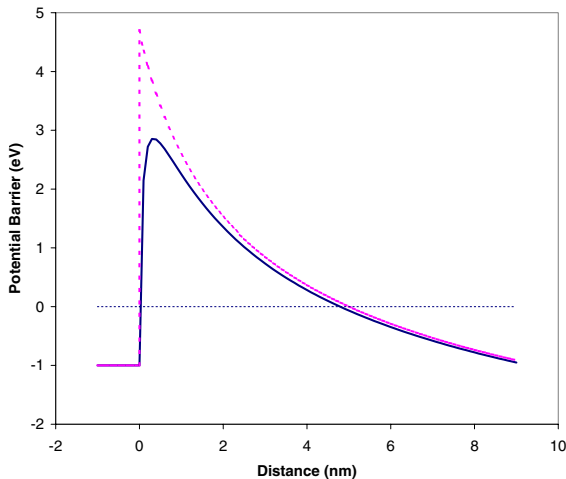


Fig. 3. Shape of the potential barrier plotted perpendicularly to the boundary element at the apex of a CNT with (solid line) and without (dashed line) image charge potential. The work function is  $W = 4.7$  eV, the height and radius of the CNT are  $H = 2 \mu\text{m}$  and  $R = 2$  nm, respectively

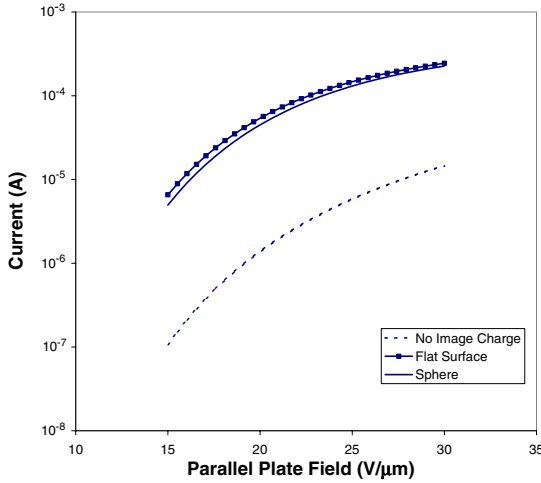


Fig. 4. Emission current from a CNT ( $H = 2 \mu\text{m}$ ,  $R = 2 \text{nm}$ ) as a function of the parallel plate field with three different options for the image charge potential

curve in Fig. 3, decreases as the distance to the apex increases. For this reason it is important to use the actual barrier to accurately calculate the field emission current. Indeed, a triangular barrier using the electric field at the surface would lead to a considerable overestimate of the emitted current.

Figure 4 displays the current–voltage characteristic for a CNT with height  $H = 2 \mu\text{m}$  and radius  $R = 2 \text{nm}$ . The results of three calculations are compared. A barrier without image charge potential is used in the first calculation. In the second and third calculations, the image charge potential for a flat surface and for a sphere of radius  $R$ , respectively, are used. The difference between the two flavors of image charge potential is very small compared to the difference to the case without image charge effects. This result agrees with earlier calculations [4] and we believe that it is acceptable to use the image charge potential for a flat surface in further calculations. We have also parameterized the  $I$ – $V$  curves with a formula that extends the Fowler-Nordheim formula to CNT emitters; these results will be presented in another publication.

One of the issues in producing CNT films for FED applications is the mutual screening of neighboring CNT that reduces the field enhancement factor. Nilsson et al. [8]

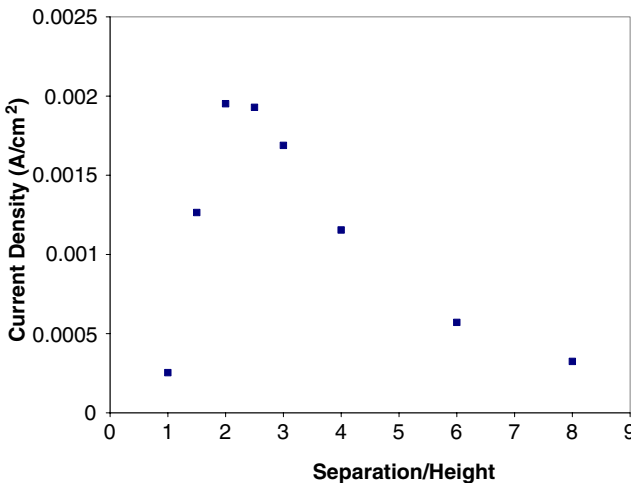


Fig. 5. Emission current density from a hexagonal array of CNTs as a function of their separation

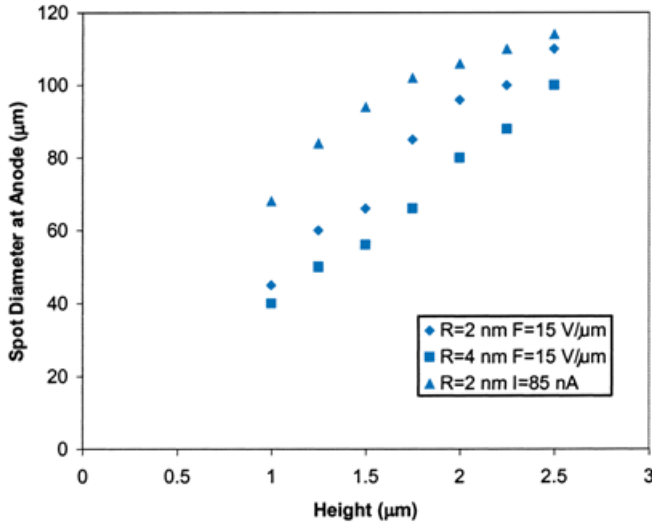


Fig. 6. Diameter of the emission spot for an anode to cathode separation of 0.7 mm

have recently presented experimental results on screening effects correlated with 2D simulations. In Fig. 5 we present the current density as a function of the separation between CNTs arranged on a hexagonal lattice and oriented perpendicularly to the surface. The height of the CNTs is  $H = 0.5 \mu\text{m}$ . As already mentioned in Ref. [8], the current density features a maximum that results from two opposing trends. The first trend is that the field at the apex of the CNT and hence the emitted current increase as the separation increases because the screening effects fade away. The second trend is that the current density decreases as the separation increases because the number of CNT per unit area decreases. It should be noted that the rising slope is dominated by the exponential dependence of the emission current on the electric field whereas the decreasing slope is determined by the area term in the denominator of the current density expression.

The final issue that we address is the lateral spread of the emitted electrons. This parameter is of great importance when building a FED because it determines the spot size on the phosphorescent anode and ultimately the size of the pixel. Figure 6 displays the diameter of the spot as a function of the height of the CNT for a cathode to anode separation of 0.7 mm. Two of the three curves are for CNTs with two different radii and for the same parallel plate field; the spot diameter in these two cases increases approximately at the same rate with the CNTs with the smaller radii yielding a slightly larger spot size. The lateral spread is determined by the region in which the electric field has a finite lateral component that causes an increase of the lateral velocity. While it can be argued that it is the magnitude of the electric field in this region that determines the increase of the spot size we have shown that it is its extension that is the dominant factor. The third curve in Fig. 6 supports this statement. If for each height the voltage is adjusted so that the emitted current is the same, the spot size still increases with the CNT height. A plot of the electric field lines shows that the reason for this increase mainly lies in the increase of the size of the region where the electric field has a finite lateral component.

#### 4. Conclusion

We have presented results that set the basis for a FED design tool. Our results are based on a continuum description of the CNT and on the locally 1D approximation for the emission current calculation. We have investigated the effects of the image charge potential, screening and lateral spread as a function of the height and radius of the CNT. In a later work we will present our parametrization of the  $I$ - $V$  characteristics and results using the Bardeen transfer Hamiltonian technique to include atomic level effects.

#### References

- [1] W. B. CHOI, D. S. CHUNG, J. H. KANG, H. Y. KIM, Y. W. JIN, I. T. HAN, Y. H. LEE, J. E. JUNG, N. S. LEE, G. S. PARK, and J. M. KIM, *Appl. Phys. Lett.* **75**, 3129 (1999);  
Motorola Advanced Display Technology Lab., unpublished.
- [2] J. BARDEEN, *Phys. Rev. Lett.* **15**, 57 (1961).
- [3] R. RAMPRASAD, L. R. C. FONSECA, and P. VON ALLMEN, *Phys. Rev. B* **62**, 5216 (2000).
- [4] P. H. CUTLER, J. HE, J. MILLER, N. M. MISKOVSKY, B. WEISS, and T. E. SULLIVAN, *Prog. Surf. Sci.* **42**, 169 (1993).  
K. L. JENSEN, to be published.
- [5] *Handbook of Grid Generation*, Eds. J. F. THOMPSON, B. K. SONI, and N. P. WEATHERILL, CRC Press, Boca Raton (FL) 1999.
- [6] L. R. C. FONSECA, P. VON ALLMEN, and R. RAMPRASAD, *J. Appl. Phys.* **87**, 2533 (2000).
- [7] J. D. JACKSON, *Classical Electrodynamics*, Wiley, New York 1975.
- [8] L. NILSSON, O. GROENING, C. EMMENEGGER, O. KUETTEL, E. SCHALLER, and L. SCHLAPBACH, *Appl. Phys. Lett.* **76**, 2071 (2000).

